Proceedings of the Canadian Society for Mechanical Engineering International Congress 2021
CSME Congress 2021
June 27-30, 2021, Charlottetown, PE, Canada

A RADIAL BASIS FUNCTION ARTIFICIAL NEURAL NETWORK METHODOLOGY FOR SHORT AND LONG FATIGUE CRACK PROPAGATION

S.N.S. Mortazavi, A. Ince*
Department of Mechanical, Industrial and Aerospace Engineering, Concordia University, Montreal, Canada
*ayhan.ince@concordia.ca

Abstract—Fatigue damage process inherently has multiscale characteristics. As a result, fatigue cracks mainly classified as short cracks (SCs) and long cracks (LCs). It is necessary to quantify the fatigue crack growth (FCG) rate in both the short and long crack regimes. Especially in the case of lightweight alloys and high cycle fatigue in which short cracks' behavior dominates total fatigue life. There is still no proper model to characterize FCG rate in the SC regime. In the presented study, a radial basis function artificial neural network (RBF-ANN) model as a machine learning approach has been developed to quantify the FCG rate in both the SC and LC regimes. Experimental data sets of 2024-T3 and 7075-T6 aluminum alloys are employed to train and verify the model. The presented study showed that the RBF-ANN model can accurately predict the nonlinearity of FCG rate in terms of stress intensity factor range in both the SC and LC regime. However, the predictions showed that the extrapolation ability of the model is not as appropriate as its interpolation capability. In addition, density and distribution of the input data strongly affect the accuracy of the RBF-ANN model.

Keywords: short crack; long crack; machine learning; neural network, fatigue crack growth

I. INTRODUCTION

Fatigue crack growth (FCG) should be investigated in different scales. As Kitagawa- Takahashi type diagram [1] suggests, fatigue cracks are classified as short cracks (SCs) and long cracks (LCs). In addition, SCs can be divided as microstructurally short cracks and physically short cracks [2]. Linear elastic fracture mechanics (LEFM) method has been developed to quantify FCG rates mainly in LC regime. However, it is widely accepted that SC regime dominates total fatigue life at lower stress levels [2]. The most famous LEFM method was proposed by Paris and Erdogan [3] as follows:

$$da / dN = C(\Delta K)^m \tag{1}$$

Where da/dN is the FCG rate, ΔK is the stress intensity factor (SIF) range, and C and m are materials constants. One of the most important shortcomings of Paris and Erdogan model is that it cannot account for stress ratio (R-ratio). As a result, this model has been received many modifications. Many of such modifications are based on crack closure concept such as the ones suggested by Elber [4] and Newman [5]. However, there is still an ambiguity that if crack closure is really an important controlling parameter in the SC regime or even in the LC regime. Another group of such modifications is based on the "Unified Approach" introducing two controlling parameters to quantify FCG rates [6]. Noroozi et al. [7] introduced UniGrow model and showed that an appropriate two-parameter driving force model can account for stress ratio in the LC regime. However, Bang et al. [8] demonstrated that UniGrow model has a substantial deficiency to quantify FCG in the SC regime. The substantial point is that most of all mentioned models introduced a mathematical function such as "*f*" shown in (2) to quantify FCG rate in the LC regime. The function "*f*" depends on two controlling parameters (ΔK and R-ratio). On the other hand, it has been widely accepted that in the case of SC regime, FCG rate depends on three controlling parameters which are ΔK, stress level (σ) and R-ratio [2]. As a result, the function "*f*" in (2) can be replaced by function "*g*" in the case of SC regime as shown in (3).

$$da / dN = f(\Delta K, R) \tag{2}$$

$$da / dN = g(\Delta K, R, \sigma) \tag{3}$$

The aim of almost all models given in literature is to stablish a mathematical expression like (2) or (3). Although UniGrow model showed a noticeable improvement to characterize behavior of LCs, there is still no proper model to account for the SC regime. The reason is that the number of controlling parameters affecting FCG rate simultaneously are more than that which were considered in previous models given in literature. Recently, artificial neural network (ANN) algorithms as machine learning methods, which can account for many variables, received a great interest in the fatigue failure area [9-13]. However there has been no investigation to employ such approaches to quantify FCG rate in the SC regime. In the presented study, a radial basis function artificial neural network

(RBF-ANN) method is developed to characterize FCG rate in both the short and long crack regime. In other words, an RBF-ANN model is developed to come up with a function like "*f*" and "*g*" in (2) and (3) for the long and short crack regime, respectively. To train and verify the model experimental data sets of 2024-T3 and 7075-T6 aluminum alloys are employed.

II. MODELIN METHODOLOGY

A. *Radial basis function artificial neural network*

RBF-ANN suggests that every point in a particular data set influences the value of the hypothesis at an arbitrary point based on the distance between the point and the hypothesis. In the presented study, Gaussian function is employed to quantify such influence. Gaussian function is shown in Fig. 1 schematically. As shown in Fig. 1, the influence decreases gradually by increasing the distance from the center of the bump as the coordinates of the hypothesis. With all these in mind, the hypothesis can be defined as follows:

$$h(x) = \sum_{k=1}^{K} w_k exp(-\gamma \|X - \mu_k\|^2) + b_k \;\; and \; K \leq N \quad (4)$$

Where N is the number of data, k is the number of radial basis functions, b is named bias, μ_k are the center of each activation function, w_k are called weights, and γ is a positive constant called spread of radial basis function (SRBF). As shown in Fig. 1, SRBF indicates how sharp the influence changes through the distance. As shown in Fig. 2, RBF-ANN consists of three layers. The first layer embraces the input data (X_i). The model generates K subdomains and determines a center (μ_i) to each of them. The second layer includes the activation functions receiving the distance between each input data and their corresponded centers. The third layer embraces the output data. The developed model needs to solve the equation shown in (4) for all the input data. That is to say, N equations consisting K unknown, in which $K \leq N$, is solved simultaneously in order to calculate b_i and w_i. It should be noticed that RBF-ANN is a feedforward static neural network.

B. *Charactrizing fatigue crack growth rate by the means of artificial neural network*

As discussed earlier, FCG rate can be expressed by a function of "*f*" shown in (2) depending on two controlling parameters in the LC regime.

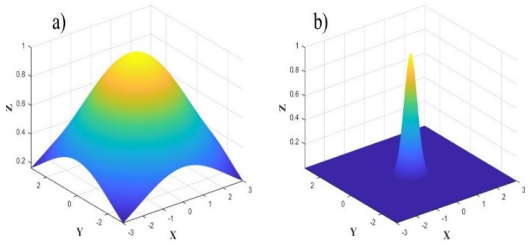

Fig. 1. The influence of SRBF on Gaussian Function. a) High SRBF and b) low SRBF

However, FCG rate can be quantified by a function like "*g*" shown in (3) depending on three controlling parameters in the SC regime. With this in mind, two separate RBF-ANN are developed to quantify FCG rate in the LC and SC regime. The first model is intended to provide a function of "*f*" shown in (2) in the case of LC regime. As a result, the first model is a two-input single-output RBF-ANN. It means, the first model receives ΔK (SIF range) and R-ratio (stress ratio) as the input and da/dN (FCG rate) as the output. In other words, X_1 is (ΔK_1, R_1), X_2 is (ΔK_2, R_2), etc. in Fig. 2. The second model is developed to calculate FCG rate in the SC regime. However, since the number of data in the case of SC regime is limited in the literature, SC regime is investigated in a constant R-ratio. One may realize that if R-ratio is considered as a constant, FCG rate in the SC regime can be quantified by a function like "g^*" depending on ΔK and σ (stress level) as shown in (5):

$$\frac{da}{dN} = g(\Delta K, R, \sigma) \xrightarrow{if: R=constant} \frac{da}{dN} = g^*(\Delta K, \sigma) \quad (5)$$

As a result, the second model is a two-input single-output RBF-ANN. This model takes ΔK and σ as the input and da/dN as the output while R-ratio is kept as a constant. In this case, X_1 is (ΔK_1, σ_1), X_2 is (ΔK_2, σ_2) in Fig. 2. The procedure employed to develop the models is explained as follows: First, the logarithm of ΔK and da/dN is taken to decrease the scatter influence caused by order of the magnitude. Then all of them are normalized. Afterward, the RBF-ANN models are trained by the means of toolbox of MATLAB R2018b software. In the presented study 30% of data were used to verify the model. It means, software uses 70% of data to train the model and then employ 30% of them to verify if the number of neurons, weights and biases are appropriately calculated. If the prediction results are not accurate enough, software adjusts the mentioned values until acceptable results are achieved. The latter step is taken by software automatically. In the next step the predicted results are compared with the experimental ones. If the results of interpolation or extrapolation are not accurate enough, the user needs to adjust SRBF manually. According to the Fig. 1, one may realize that a high SRBF provides a relatively better extrapolation. On the other hand, a low SRBF results accurate interpolation. As a result, the user needs to balance both sides and find an optimized value of SRBF. It will be discussed that such optimized value would be achievable if the number and distribution of the data are appropriate.

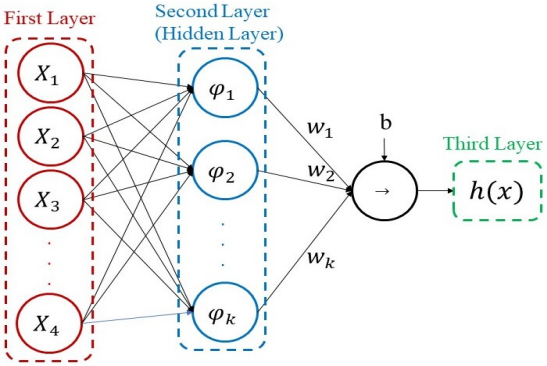

Fig. 2. The structure of RBF-ANN

III. RESULTS AND DISCUSSION

A. *Long cracks*

In order to formulate a function of "*f*" in (2) in the LC regime, FCG date in terms of ΔK and R-ratios should be fed to RBF-ANN model. In the presented study, such experimental data sets of Al7075-T6 and Al2024-T3 are employed. Fig. 3 shows the experimental data sets of the mentioned alloys in the LC regime. The experimental data sets and the corresponded experimental procedures can be found in the literature [7-1-14-15-16]. It should be emphasized that 70% of the data are randomly chosen and employed to train the network, and the 30% are used in order to verify the ANN results. Fig. 4 presents the experimental data and ANN results of Al7075-T6 in 2D and 3D views. The number of input data in this case is 365 and they are distributed under five different R-ratios. In Fig. 4 (a) the acceptable extrapolation results are indicated by blue dashed closed curves in the threshold and fracture regions. On the other hand, Fig. 4 (b) in a 2D view presents the interpolation capability of the model. The agreement between experimental data and ANN interpolation results shows that RBF-ANN is able to predict the nonlinearity of FCG rates in terms of ΔK under different R-ratios.

Fig. 5 presents the experimental data and ANN results for 2024-T3 aluminum alloy. The number of input data in this case is 93 under five different R-ratios as shown in Fig. 3 (b). Fig. 5 (b) shows an excellent agreement between the experimental data and ANN results. That is to say, RBF-ANN model can interpolate accurately in the case of Al2024-T3 as well as Al7075-T6. However, in Fig. 5 (a) there is no extrapolation results. It means, in the case of Al2024-T3, the RBF-ANN model is not able to predict the behavior of FCG rate in the regions, in which there is no input data in hand. One may realize that in the case of Al7074-T6 (see Fig. 4), in which the number of data is 365, the developed RBF-ANN model is able to interpolate and extrapolate simultaneously. However, since the number of input data decreases from 365 to 93 in the case of Al2024-T3, the model can only interpolate accurately. It should be noticed that even in the case of Al2024-T3, an acceptable extrapolation is achievable by increasing the SRBF value. However, that results a poor interpolation. As shown in Fig. 1 (a) a relatively high spread of radial basis function is suitable to have an accurate extrapolation. The reason is that the hypothesis can receive influence from the input data in a larger distance. As a result, FCG rate in an arbitrary point can be predicted based on the input data in a larger distance.

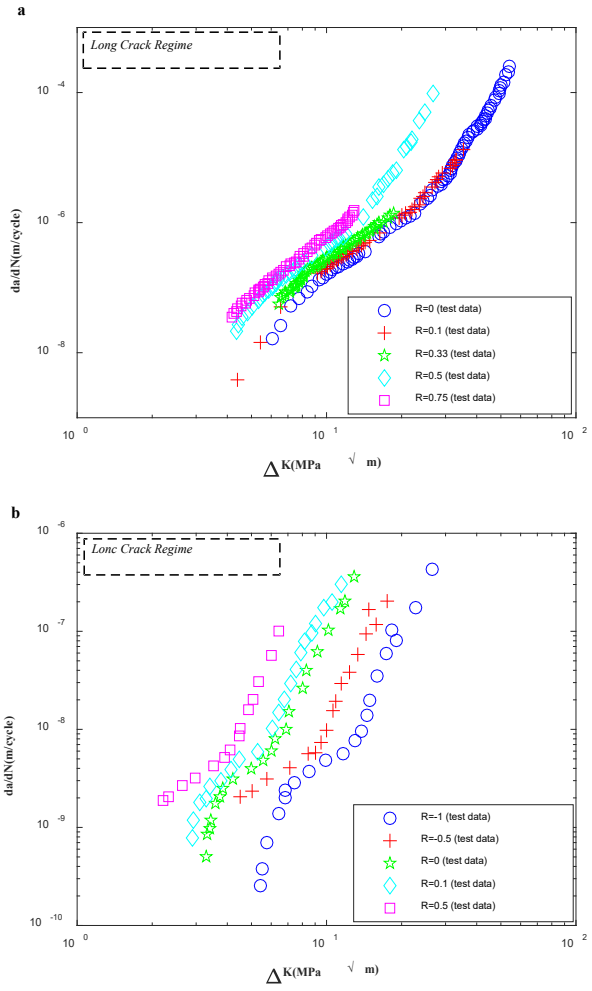

Fig. 3. FCG data in LC regime of a) Al7075-T6 and b) Al2024-T3.

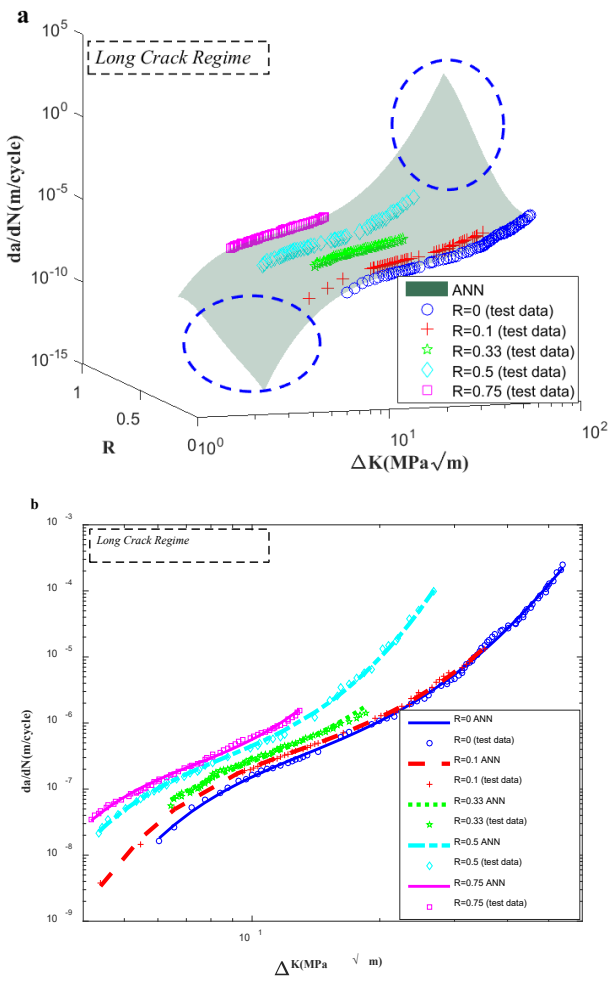

Fig. 4. LCs experimental data and corresponded ANN results of Al7075-T6 in a) 3D view and b) 2D view.

On the other hand, a relatively low SRBF as shown in Fig. 1 (b) is suitable for interpolation. As shown in Fig. 1 (b) the influence on hypothesis sharply decreases through the distance. It means, only local input data can be employed to predict the FCG rate in an arbitrary point. With all these in mind, an optimized SRBF is required to have an acceptable extrapolation and interpolation simultaneously. However, such optimized value of SRBF is achievable if the number and the distribution of the input data are appropriately selected.

B. Short cracks

As discussed earlier, FCG can be characterized by three controlling parameters (ΔK, σ, and R-ratio) in the SC regime. However, since the number of input data in the literature is limited in the case of SC regime, in the presented paper FCG rates are investigated under a constant R-ratio. In other means, the aim is to come up with a function of "g*" under a constant R-ratio rather than a function of "g" in (3). As a result, FCG data in terms of ΔK and maximum stress level (σ) is required in order to train and verify the RBF-ANN model in SC regime. Such data sets and the corresponded experimental procedure is accessible in literature [1,17-22].

Those data sets are presented in Fig. 6 for 7075-T6 and 2024-T3 aluminum alloys. The R-ratio is kept constant and it equals 0.0 and 0.5 for Al7075-T6 and Al2024-T3, respectively. In this section, 70% of the input data is utilized to train the network and 30% of them is employed to verify the results as well as the previous section as per LC regime. Fig. 7 presents the experimental data and ANN results in the SC regime for the 7075-T6 aluminum alloy under a constant R-ratio in 3D and 2D views. As shown in this figure an acceptable agreement between experimental data and ANN results is achieved. However, the RBF-ANN model is not able to predict the nonlinearity of FCG rates on the basis of ΔK and maximum stress level (σ). The reason is that the input data is distributed under only two stress levels (σ=120 MPa and σ=140 MPa). In other words, the number of data points in both the ΔK and σ direction is important. It is obvious that only a line would fit between two points. To produce a nonlinear function at least three points are required. As a result, the input data should be distributed at least under three maximum stress levels to predict the nonlinearity of FCG rates in terms of stress intensity factor (SIF) range and maximum stress level. That is to say, in addition to the number of input data, the distribution of the input data is also important.

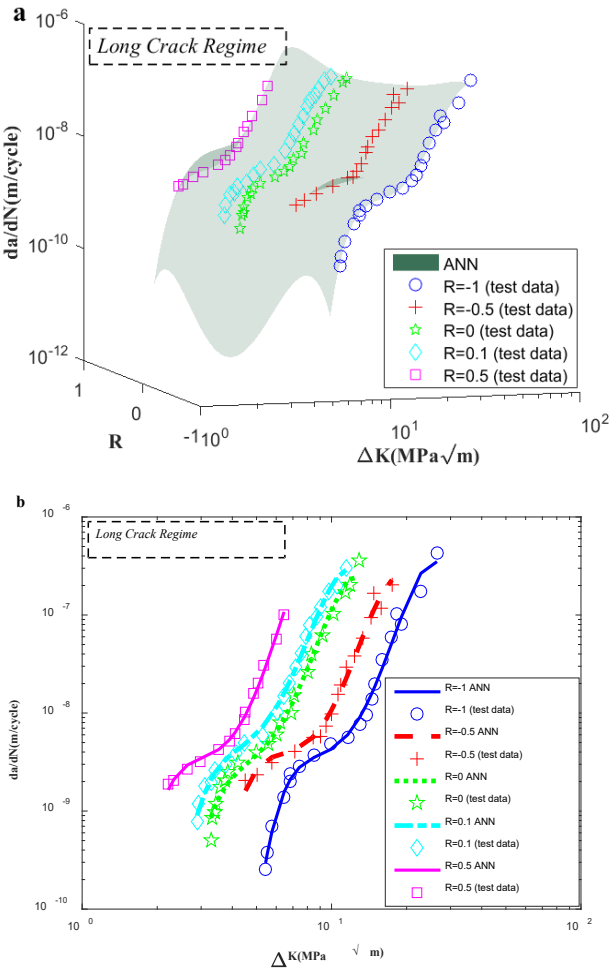

Fig. 5. LCs experimental data and corresponded ANN results of Al2024-T3 in a) 3D view and b) 2D view.

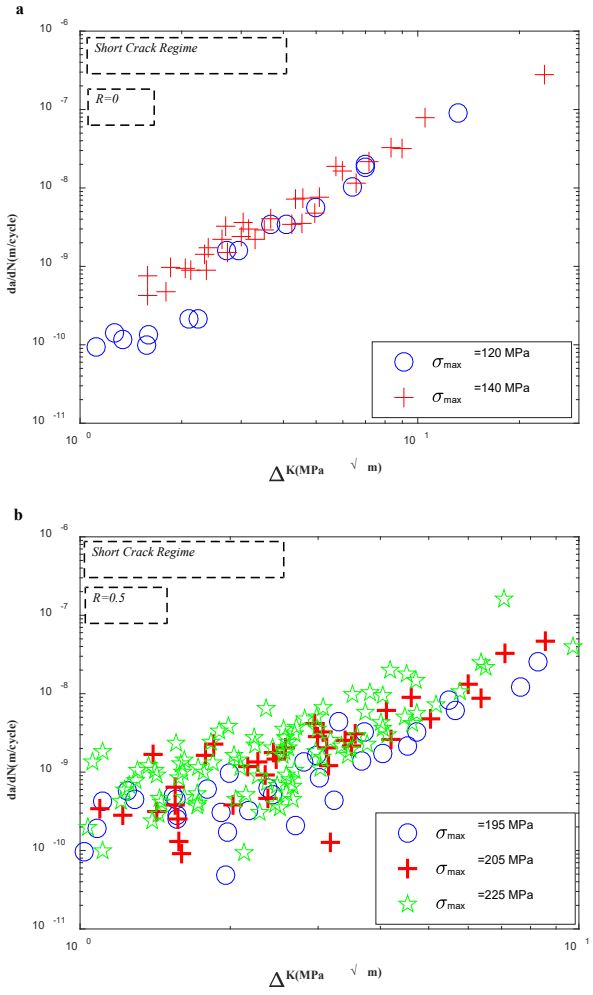

Fig. 6. FCG data in SC regime under constant R-ratio of a) Al7075-T6 and b) Al2024-T3.

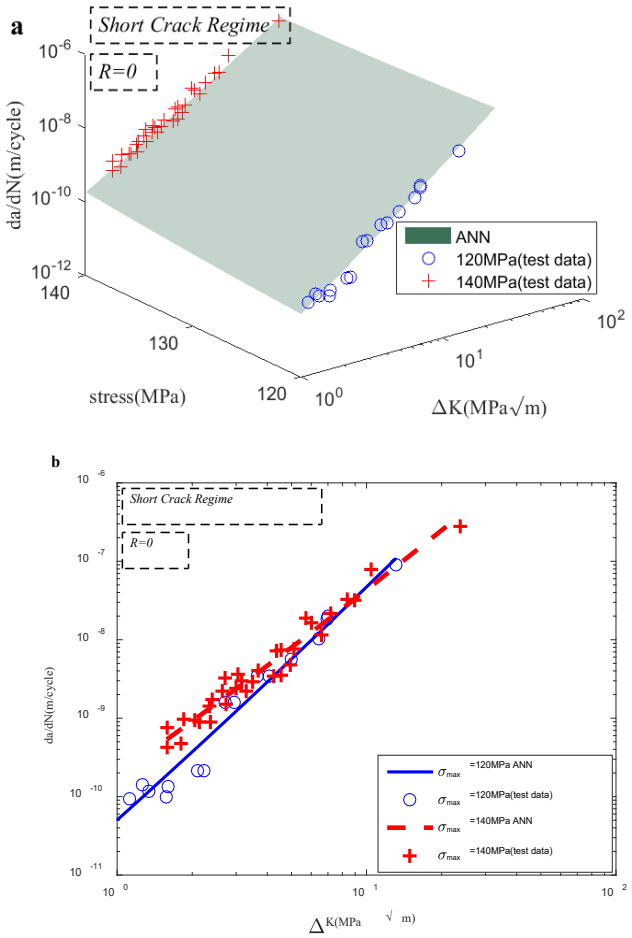

Fig. 7. SCs experimental data and corresponded ANN results of Al7075-T6 in a) 3D view and b) 2D view.

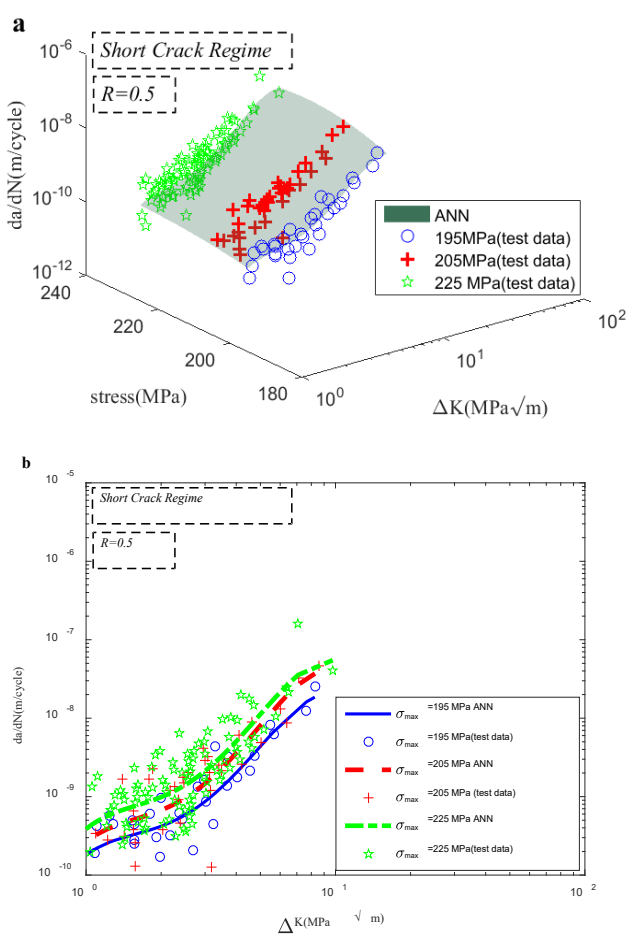

Fig. 8. SCs experimental data and corresponded ANN results of Al2024-T3 in a) 3D view and b) 2D view.

Fig. 8 shows the experimental data and ANN results in the SC regime for the Al2024-T3 under a constant R-ratio in 3D and 2D views. Since the number of input data is higher than that of Al7075-T6 and the input data are distributed under three different maximum stress levels (σ), RBF-ANN can predict the nonlinearity of FCG rate in terms of SIF range and stress level.

C. Prediction accuracy

In the presented study, probability density function (PDF) is employed to investigate the accuracy of RBF-ANN model in the short and long crack regimes. The PDF calculates the difference between the predicted and experimental FCG rate as the error values. Normal probability distribution is utilized to present the error distribution and fit PDFs. Positive and negative error values are corresponded to conservative and non-conservative prediction, respectively. Fig. 9 presents the error PDFs for Al7075-T6 and Al2024-T3 in the LC regime under various R-ratios. Error distribution of PDFs proves that the developed RBF-ANN can accurately predict FCG behavior in the LC regime, however prediction performance still relies on the sufficiency of the experimental data [23].

Fig. 10 shows the error PDFs for 7075-T6 and 2024-T3 aluminum alloys under a constant R-ratio and different stress levels in the SC regime. Although FCG data are significantly scattered, the error PDFs show the acceptable agreement between RBF-ANN predictions and experimental data under all stress levels in the SC regime.

I. CONCLUSION

In the presented study a machine learning RBF-ANN algorithm is employed to quantify FCG rate in both the SC and LC regime. The algorithm is based on the radial basis function artificial neural network method. To train and verify the model experimental data sets of 2024-T3 and 7075-T6 aluminum alloys are utilized. The results indicate that RBF-ANN has a strong capability of interpolation to predict the nonlinearity of fatigue crack growth rate in both the short and long crack regime. However, the extrapolation capability of investigated approach is not as potent as its interpolation ability. The efficiency of the proposed model dramatically depends on sufficient and distribution of training data sets.

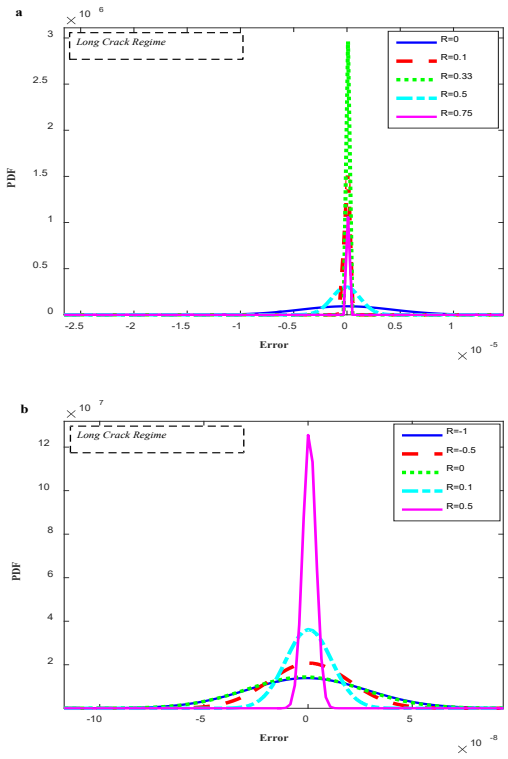

Fig. 9. Probability density function (PDF) of prediction error in LC regime for a) Al7075-T6 and b) Al2024-T3.

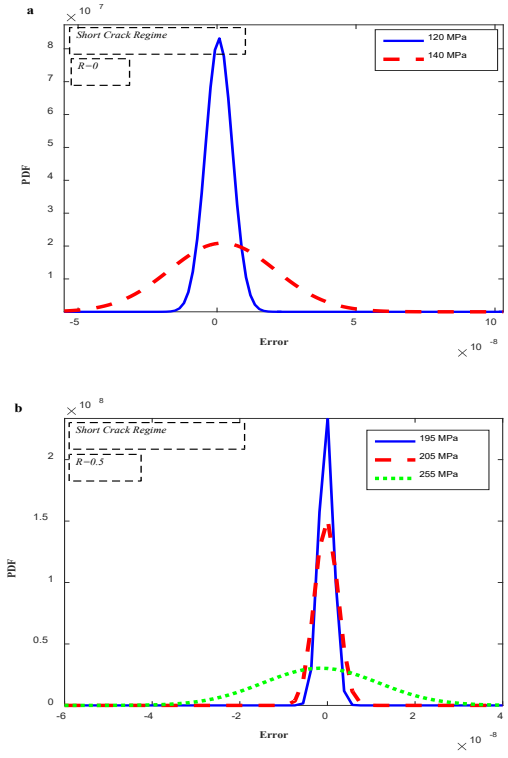

Fig. 10. Probability density function (PDF) of prediction error in SC regime for a) Al7075-T6 and b) Al2024-T3.

REFERENCES

[1] D. Bang, A. Ince, M. Noban, "Modeling approach for a unified crack growth model in short and long fatigue crack regimes", Int. J. Fatigue, vol. 128, 105182, 2019.

[2] K. Sadananda, M.N. Babu, A. Vasudevan, "A review of fatigue crack growth resistance in the short crack growth regime", Mater. Sci. Eng., A, vol. 754, pp. 674–701, 2019.

[3] P. Paris, F. Erdogan, "A critical analysis of crack propagation laws", J. Basic Eng., vol. 85, pp. 528‑533, 1963.

[4] W. Elber, "The significance of fatigue crack closure, Damage tolerance in aircraft structures", ASTM International, pp. 230‑242, 1971.

[5] J. Newman, "Prediction of fatigue crack growth under variable-amplitude and spectrum loading using a closure model", Design of fatigue and fracture resistant structures, ASTM International, pp. 255‑277, 1982.

[6] A. Vasudeven, K. Sadananda, N. Louat, "A review of crack closure, fatigue crack threshold and related phenomena", Mater. Sci. Eng., A, vol. 188, pp. 1‑22, 1994.

[7] A. Noroozi, G. Glinka, S. Lambert, "A study of the stress ratio effects on fatigue crack growth using the unified two-parameter fatigue crack growth driving force", Int. J. Fatigue, vol. 29, pp. 1616‑1633, 2007.

[8] D. Bang, A. Ince, L. Tang, "A modification of UniGrow 2-parameter driving force model for short fatigue crack growth", Fatigue Fract. Eng. Mater. Struct., vol. 42, pp. 45‑60, 2019.

[9] J.-Y. Kang, J.-H. Song, "Neural network applications in determining the fatigue crack opening load", Int. J. Fatigue, vol. 20, pp. 57‑69, 1998.

[10] V. Venkatesh, H. Rack, "A neural network approach to elevated temperature creep‑fatigue life prediction", Int. J. Fatigue, vol. 21, pp. 225‑234, 1999.

[11] T.T. Pleune, O.K. Chopra, "Using artificial neural networks to predict the fatigue life of carbon and low-alloy steels", Nucl. Eng. Des., vol. 197, pp. 1‑12, 2000.

[12] P. Artymiak, L. Bukowski, J. Feliks, S. Narberhaus, H. Zenner, "Determination of S-N curves with the application of artificial neural networks", Fatigue Fract. Eng. Mater. Struct., vol. 22, pp. 723‑728, 1999.

[13] H. Wang, W. Zhang, F. Sun, W. Zhang, "A comparison study of machine learning based algorithms for fatigue crack growth calculation", Materials, vol. 10, 543, 2017.

[14] W. Zhang, Z. Bao, S. Jiang, J. He, "An artificial neural network-based algorithm for evaluation of fatigue crack propagation considering nonlinear damage accumulation", Materials, vol. 9, 483, 2016.

[15] A. Noroozi, G. Glinka, S. Lambert, "A two parameter driving force for fatigue crack growth analysis", Int. J. Fatigue, vol. 27, pp. 1277‑1296, 2005.

[16] X. Huang, T. Moan, "Improved modeling of the effect of R-ratio on crack growth rate", Int. J. Fatigue, vol. 29, pp. 591‑602, 2007.

[17] J. Newman, X. Wu, M. Swain, W. Zhao, E. Phillips, C. Ding, "Small-crack growth and fatigue life predictions for high-strength aluminium alloys. Part II: crack closure and fatigue analyses", Fatigue Fracture Eng. Mater. Struct., vol. 23, pp. 59‑72, 2000.

[18] P. Edwards, J.C. Newman Jr, "Short-crack growth behaviour in various aircraft materials", AGARD-R-767, Neuilly-sur-Seine, France, 1990.

[19] J. Newman Jr, "Analyses of Fatigue and Fatigue-Crack Growth Under Constant-and Variable-Amplitude Loading", Mechanics of Materials Branch NASA Langley Research Center Hampton, Virginia USA, 1999.

[20] K. Wang, F. Wang, W. Cui, T. Hayat, B. Ahmad, "Prediction of short fatigue crack growth of Ti-6Al-4V", Fatigue Fract. Eng. Mater. Struct., vol. 37, pp. 1075‑1086, 2014.

[21] R. Cook, "The Growth of Short Fatigue Cracks in an Aluminium Alloy", Technical Report, Farnborough, Hampshire, November, 1992.

[22] D. Bang, A. Ince, "A short and long crack growth model based on 2-parameter driving force and crack growth thresholds" International Journal of Fatigue, vol. 141: 105870, 2020.

[23] S. Mortazavi and A. Ince, "An artificial neural network modeling approach for short and long fatigue crack propagation," Computational Materials Science, vol. 185, p. 109962, 2020